ARMA 15-0102

SAND2015-1413C

Proppant and host rock deformation in fractured shale flow through experiments

Ingraham, M.D., S.J. Bauer, E.C. Quintana, D. Bolintineau, R.R. Rao, J.B. Lechman

Sandia National Laboratories, Albuquerque, NM, USA

This paper was prepared for presentation at the 49th US Rock Mechanics / Geomechanics Symposium held in San Francisco, CA, USA, 28 June-1 July 2015.

ABSTRACT: A series of tests were performed on a manually fractured (subparallel to bedding) and propped (using quartz sand) shale plug to determine the extent to which the proppant fractured and the effect the proppant had on the fracture wall when subjected to reservoir conditions. The specimen was repeatedly subjected to reservoir conditions of 20.7 MPa confining pressure, 6.9 MPa differential stress and a temperature of 75°C. While at reservoir conditions the sample permeability was measured. Periodically the specimen was removed from the test system and scanned with a X-ray micro computed tomography machine to visualize the fracture and proppant. Noticeable decrease in flow was observed with subsequent testing due to fracture closure. This can be attributed to observations of clay swelling, proppant embedment/fracture, and shale wall spalling leading to a decrease in effective fracture aperture. Flow induced particle transport clogged flow paths and impeded flow. It was observed that isolated grains tended to crush whereas continuous grain patches tended to fracture with little displacement and tended towards embedment.

1. INTRODUCTION

In recent years the United States has become the largest producer of both petroleum and natural gas. This is a direct result of source rock exploitation through drilling and hydraulically fracturing long horizontal bore holes. While there is no dispute that this process has been effective and profitable there is still much that is not well understood about the life of proppants and fracture connectivity downhole. Production declines from these sources are higher than conventional wisdom predicts. Therefore, it is important to better understand the fracture and proppant placement process so that it can be tailored to help maximize production while minimizing environmental impact.

This work seeks to provide an experimental basis for the development of models of permeability and particle transport that account for the small fracture apertures likely present in the subsurface. In particular, when the particle size is comparable to the crack aperture, particle geometry must be modeled explicitly, leading to complex geometries with high aspect ratios. The computational meshes used are taken directly from the crack geometry determined by X-ray micro computed tomography (μCT) scans of the specimens.

2. BACKGROUND

The fundamental work on permeability of geologic fractures has been performed and shows that conductivity (which is proportional to permeability) scales with the cube of half the fracture opening. These theoretical models can be scaled for surface roughness [1] and obstructions modeled as a bed of nails [2]. Fracture data can be manipulated into these frameworks; however, determining the fracture roughness and obstruction of a hydraulic fracture in the field is difficult if not impossible. Therefore it is suggested that more laboratory testing is needed that seeks to more closely replicate the field conditions.

Proppant placement and the ability of proppant to maintain permeability in a fracture has been studied extensively through field studies which look at the effectiveness of proppant injection at increasing production from hydraulically fractured wells. There have also been extensive tests and models performed on idealized fractures, however there has been little published work seeking to perform tests which model the exact conditions with actual shale and proppant in the laboratory.

Studies investigating proppant effectiveness in the field include those which look at its feasibility in a particular basin, such as one that investigated the Marcellus shale in Pennsylvania [1]. It was determined that hydraulic fracturing was a feasible means for increasing recovery while posing a minimal hazard to ground water supplies in the region. Also, investigations have looked at the effectiveness of proppant injection by examining flow back from fractured wells [2]. It was found that shear

fractures have the ability to block proppant movement when fractures grow in an off-balance mode (non-planar), and that most proppant flow back is caused by gravity and flow of the reservoir fluid parallel to proppant packs.

There have been significant advances in drilling, completion and stimulation of wells over the past few years [ex. 3]. Baihly et al. noted that initial production from almost every basin they studied increased with wells completed as time progressed. The exception to this was wells which were drilled in the Barnett shale. It is suggested that this could be due to differences in the natural fractures, or non-optimal stimulation of the source rock.

One advance in the realm of stimulation is the introduction of heterogeneous deposition of proppants through a pulsing deposition processes such as the HiWAY proppant/deposition process developed by Schlumberger [ex. 4,5]. While this has been very successful in increasing productivity from the wells, the question of what exactly is happening downhole remains. Simulations of the deposition of proppant in these situations are typically based on continuum scale particle transport models that are known to be problematic when the particle size approaches the characteristic length scale of the flow geometry (in this case the particle crack aperture). In hydraulically fractured source rocks, common crack apertures are likely in the range of 1-3 particle diameters, suggesting the need for novel model development

Moving into the experimental realm, there have been some interesting studies which have looked at one particular aspect of loss of permeability in fractured shale. For example Wen et al. [6] looked at the effect of proppant density on embedment into the shale and found that embedment depended heavily on both the density of the proppant in the fracture as well as the properties of the rock the proppant was placed in. These factors combined with the closure pressure and time resulted in a reasonably predictable closure trend.

Fredd et al [7] investigated the effectiveness of proppant concentrations and shearing on maintaining permeability of hydraulic fractures. It was determined that proppant strength reduces the importance of the properties of the formation. It was also found that with sufficient shearing of the fracture it is possible to maintain permeability without large quantities of proppant due to asperities. However it is difficult to predict fracture permeability under asperity dominated conditions; therefore it is preferable to inject sufficient proppant to ensure that fracture permeability is dominated by the emplaced proppant and not the asperities.

Proppant embedment and permeability tests have also been conducted which looked at the force required to embed proppants into different types of shale and the effect that the different degrees of embedment had on the permeability of the fracture that was being held open [ex. 10]. It has been found that high clay content allows for significantly more proppant embedment, but it has been noted that along with clay quantity, clay type can be important as well as other factors such as organic content and porosity.

3. MATERIALS AND METHODS

The shale used in this work was a core plug nominally 25.4 mm in diameter and 50.8 mm in length, which contained 5-10% porosity and 10-40% clay. An image of the core plug is shown in Figure 1. The specimen was manually fractured subparallel to bedding, and a monolayer of proppant was randomly distributed over the fracture surface, see Figure 2. The specimen was then reassembled and jacketed in a polyvinyl chloride (PVC) heat shrink jacket between two steel end caps followed by a layer of ultraviolet cure polyurethane, see Figure 3. The proppant used was clean 20-30 sieve (0.60-0.85 mm) quartz sand.

Once jacketed the specimen was μCT scanned to analyze the pretest crack and proppant distribution, and proppant settling due to gravity was observed. The specimen was tested by being loaded into a 200 MPa pressure vessel that was placed into a 950 kN load frame used to generate the differential stress. The vessel was filled with Dow Corning 200 silicone oil. Once the vessel was filled the load frame applied a small load to ensure that the piston was in contact with the specimen. The vessel was then heated to the test temperature of 75°C with the vent port open to ensure that pressure did not build within the vessel due to the heating oil. Once at temperature the vessel vent was closed and the pressure increased to the test pressure of 20.7 MPa. After test pressure was reached the load frame was used to apply a

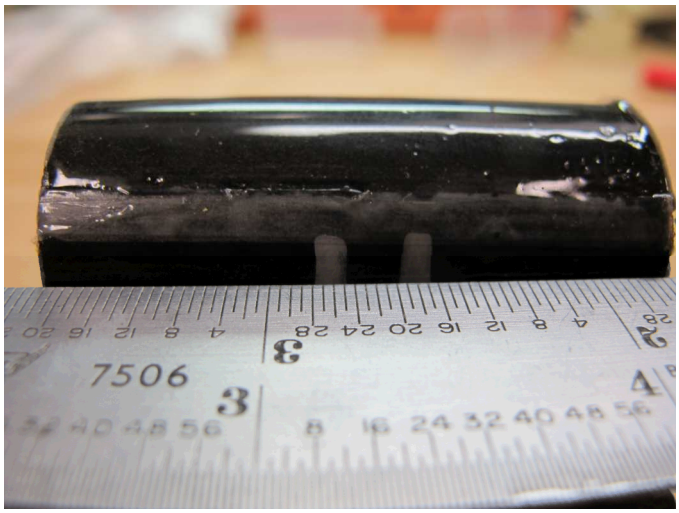

Fig. 1. Image of the solid core plug.

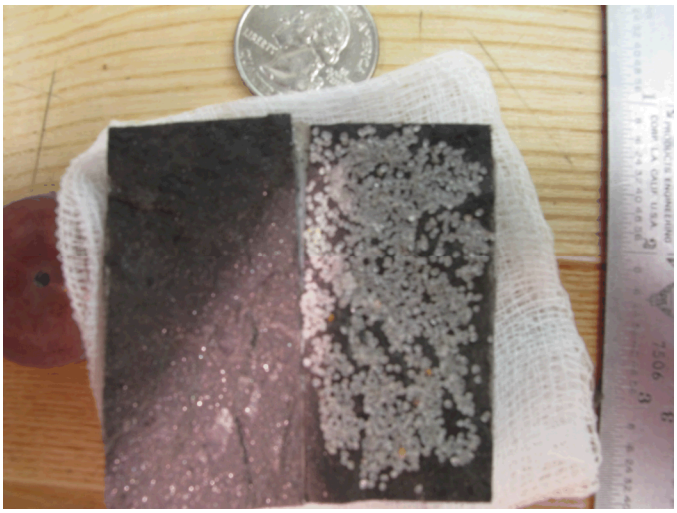

Fig. 2. Fractured sample with quartz sand proppant distributed across the surface.

differential pressure of 6.9 MPa to the specimen. After the loads were applied deionized water was introduced to the specimen at a rate of 0.002 ml/min, with the downstream vented to atmosphere. The upstream pressure was allowed to vary as necessary to maintain the flow rate.

Note that the downstream was vented out the top of the specimen, and the upstream was fed from underneath to prevent trapping of air within the pore fluid system. The constant flow was used to measure the permeability of the specimen and to see the effect that a flowing fluid would have on the shale and proppant. Brine was not used because of complications using brine in the plumbing.

The specimen was allowed to reach steady state flow, and then was held at test conditions and flowrate for 12 hours to monitor any time dependent effects. The specimen was then removed from the testing system with a procedure that was the reverse of test setup. The specimen was then placed back in the µCT scanner and re-scanned. Note that the water was not removed from the crack space between testing, therefore the majority of the crack volume during µCT scans is filled with water. This process was repeated 3 times, to develop a sense of the effect of repeated pressure cycles, and to monitor the evolution of the permeability, fracture wall integrity, and proppant life with time.

The µCT scanner used in this work was a Comet MXR-451HP/11 operated at 400kV and 3.8mA. The scanner was equipped with a Perkin Elmer XRD1620 detector with a DRZ Scintillator. The data from the scan was collected with North Star Imaging data acquisition software, and the scan took approximately 150 minutes to complete. The scan was reconstructed with Volume Graphics VG Studio Max software for reconstruction

Fig. 3. Image of the jacketed specimen with endcaps.

and 3D rendering. ImageJ was also used for some post-process analysis of µCT results.

The µCT system generates three dimensional images based on the density of the material it is imaging. This is done by imagining the specimen with an x-ray source and a specialized detector from many circumferential angles. All of these images are reconstructed with a back projection algorithm to generate a volume reconstruction of the object in terms of density. Lower density appears darker, while higher density appears lighter.

4. RESULTS AND DISCUSSION

4.1. Permeability data

The permeability data shows a strong similarity to production decline data. Figure 4 shows the evolution of the permeability of the specimen for the first test period. This curve can be modeled reasonably well with the well-known empirical Arps equation (Eq. 1). With values of $q_{gi} = 0.000278$, $b = 5.73$, $D_i = 0.002$.

$$q_g(t) = \frac{q_{gi}}{\left[1 + bD_i t\right]^{1/b}} \qquad (1)$$

The curvature parameter b is higher than normally reported for shale wells, but that could be for a number of reasons. The equation was developed for a well monitored for months and not a single fracture monitored for hours. The fracture in this testing is still somewhat idealized with reasonably constant thickness, and open end conditions. The pore fluid pressures are much lower than expected in a reservoir as in a reservoir the pore pressure would be sufficient to produce oil or gas from the shale. Also, there would be more than one fracture/fracture network generated from a number of

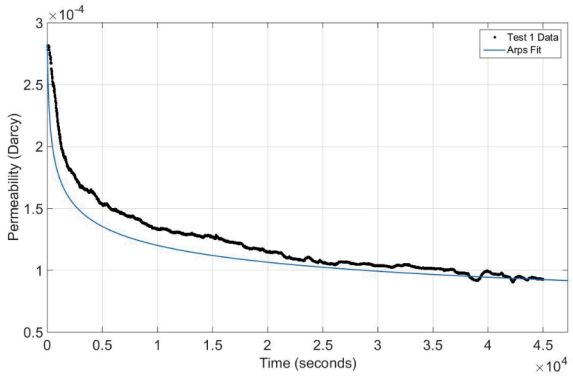

Fig. 4. Comparison of test data with Arps equation fit for the first test period. Note that the time axis was shifted to correspond with the peak of flow.

induced hydraulic fractures feeding a well which would result in higher flow and likely lower decay. The value of D_i is a little low, but not unreasonable, and the value of q_{gi} scales the curve to the initial value, which in this case is the initial permeability of the fracture, so it is not reasonable to compare values of q_{gi}.

The second test period (performed at the same conditions) shows similar results to the first, with values of q_{gi} = 0.0001, b = 3.941, D_i = 0.002. The comparison of the fit and the data can be seen in Figure 5. The third test, due to the low permeability did not show an initial spike in flow and was therefore not fit with the Arps equation. Permeability at the beginning of the second and third test periods showed good agreement with the permeability at the end of the previous test period. For example from Figure 4, at the end of the first test period, permeability was approximately $1x10^{-4}$ Darcy. This is almost exactly where the permeability started in test period 2 shown in Figure 5.

The overall evolution of permeability for the specimen is shown in Figure 6. The three points plotted represent the "steady state flow" (an average of the flowrate at the tail seen on the right side of the plot in Figures 4 and 5). Since there are only 3 data points the curve was not fit

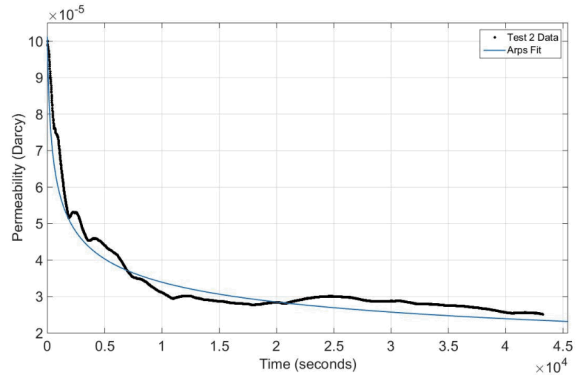

Fig. 5. Comparison of test data with Arps equation fit for the second test period. Note that the time axis was shifted to correspond with the peak of flow.

with the Arps equation, but it does show good agreement visually with the expected trend for production decline from a well.

4.2. μCT data

The μCT data was invaluable in determining the processes which were taking place to reduce the permeability in the specimen as time progressed. As expected there was some settling of the proppant particles between the initial distribution seen in Figure 2 and the test as seen in the false color μCT image in Figure 7. This image is oriented such that gravity is down. While there is noteworthy settling there is still a good distribution of proppant throughout the fracture, with some open areas, and some areas with good formation of proppant pillars. The effect this has on permeability are not entirely clear as modeling flow through this fracture is difficult due to the high number of obstructions and small aspect ratio of the crack, resulting in a complex mesh. Modeling of the flow in this fracture is currently underway. However, the settling of the proppant around the fluid inlet could be representative of a higher density proppant pack around the wellbore, resulting in some flow restriction.

Although every effort was made to ensure an even filling of the fracture volume with water when the test began there was still trapped air within the fracture space as seen in Figure 8. The dark circles in the fracture space are air bubbles that presumably formed when the specimen was filled with fluid (note that it was filled from below after being inserted into the pressure vessel). The bubbles likely formed due to surface tension effects between the proppant particles. This is brought to the reader's attention because it is likely occurring in wells when natural gas is released from the shale. In low flow situations it is possible that bubbles could become trapped within the proppant pack if there is insufficient gas flow to push the bubbles into the wellbore.

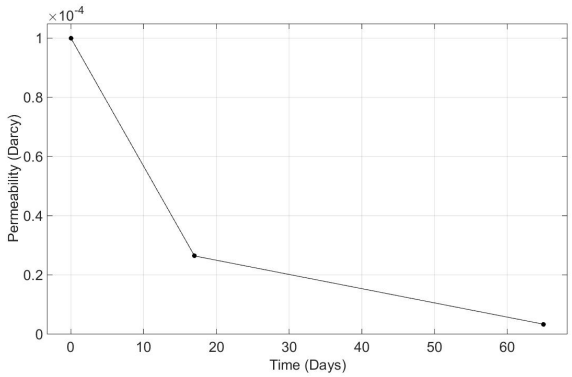

Fig. 6. Plot of permeability versus time for the permeability during the tail of the permeability vs time curves for the three tests.

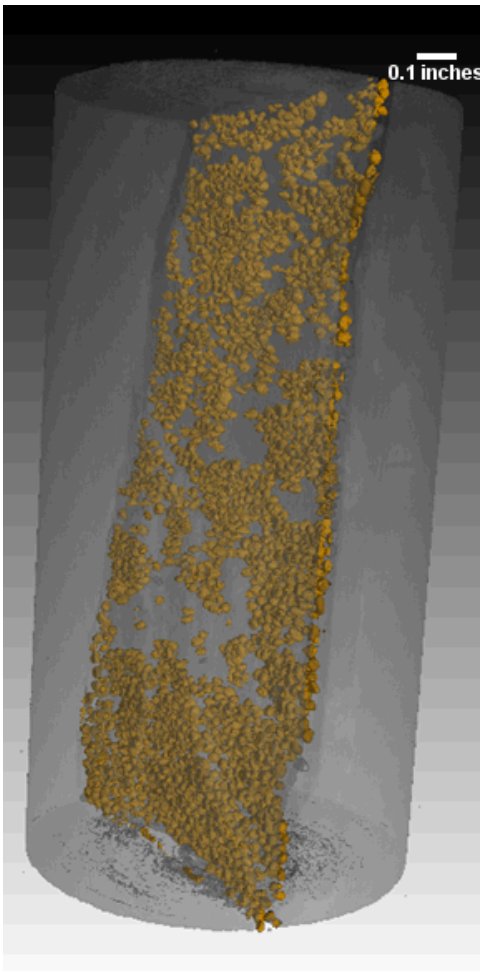

Fig. 7. A false color µCT image of the distribution of proppant within the fracture volume of the tested specimen. This image was generated after the first test.

The gas bubbles should not have a significant effect on the permeability of the fracture. Their mobility should be low due to surface tension effects between the air-water interface and the proppant particles. They are likely to remain in locations of low flow velocity and low volumetric flow rate. Therefore they should not hinder the overall fracture permeability noticeably.

Figure 9 shows the crack space after the first test in a µCT image taken parallel to the plane of the crack. The rings around the outside of the specimen are the PVC and polyurethane jackets. Things to note in this image are the grains which have fractured at relatively low confining stresses, and the shale detritus which has spalled off the fracture walls and is now floating around in the fracture void space causing clogging of flow paths. Some of the air bubbles seen in Figure 8 are also visible in this figure. It should be noted that these features were formed after approximately 18 hours under reservoir conditions, meaning that degradation of proppants and fracture walls begins to happen almost immediately after completion of a well. Proppant embedment was also observed, although it is not obvious

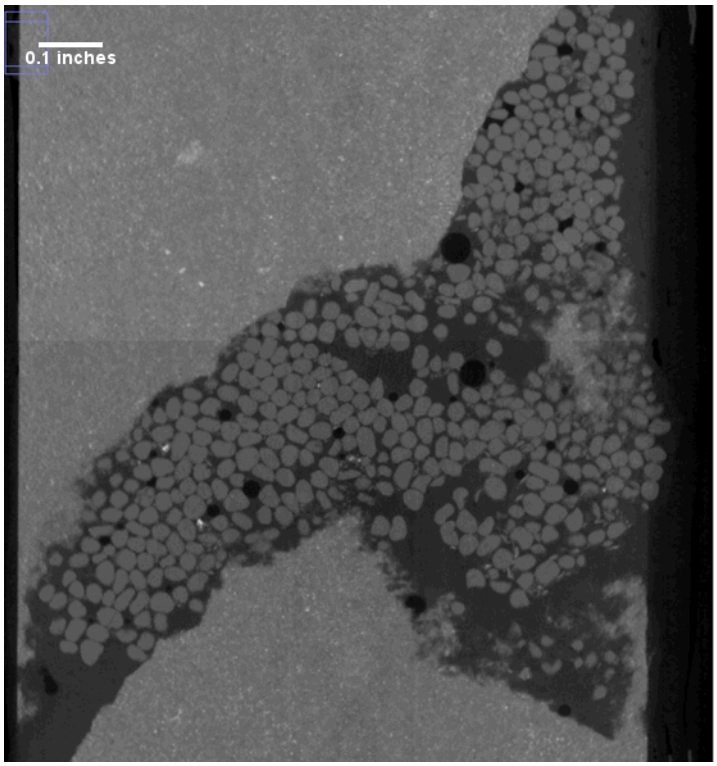

Fig. 8. µCT image of the fracture space taken roughly perpendicular to the plane of the crack. Note the black circles which are air bubbles trapped in the fracture between proppant particles. This image was taken after the first test.

in this image. Proppant embedment may have been more prominent if softer shale was used for this work [10]. It should be noted that embedded proppant particles were typically part of a proppant pillar while fractured particles were typically more isolated.

The clogging of the fracture void space only became more prominent as the specimen was tested repeatedly. Figure 10 shows the specimen after it was tested the third time, and there is significantly more shale flake in the open spaces of the fracture, as well as more proppant embedment and fractured proppant grains.

Although it is difficult to observe in the µCT images, it must be assumed that the clays in the shale are swelling when exposed to water. While the percentage of swelling clays in this particular share is relatively low, they still exist in the rock, and as a result are likely causing some reduction in the crack volume, resulting in a reduction in the permeability of the crack.

In order to determine the spacing of the crack surfaces 30 random measurements of the distance between the crack faces were taken from each µCT scan. It was found that the average fracture opening was reduced from 0.966 mm to 0.914 mm, the maximum measured fracture opening changed from 1.173 mm to 1.143 mm, and the minimum measured fracture opening changed from 0.782 to 0.686. Since the maximum opening changed much less than the minimum it implies that

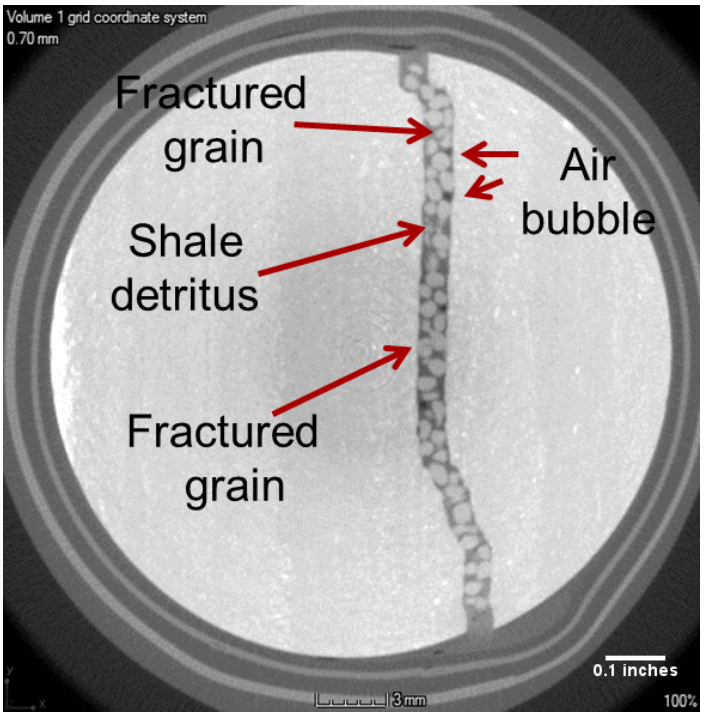

Fig. 9. µCT image of the fracture space taken parallel to the crack plane. Note the fractured grains, bubbles and pieces of shale in the crack space. This image was taken after the first test.

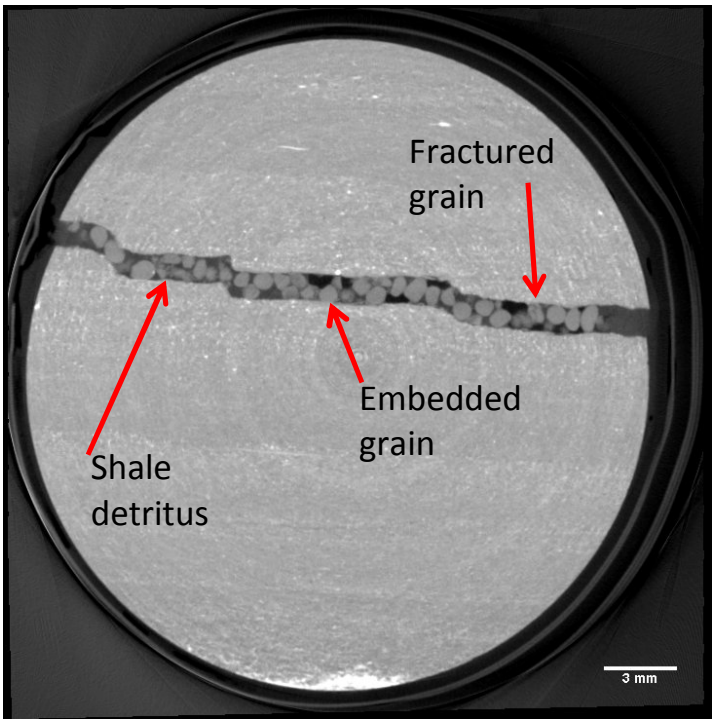

Fig. 10. µCT image of the fracture space taken parallel to the crack plane. Note the fractured grains, bubbles and pieces of shale in the crack space. This image was taken after the third test.

there is uneven closure of the fracture, likely due to the proppant which is good. A measure of the change in the crack volume would be more informative, but could not be determined within the bounds of this work.

5. CONCLUSIONS

This work shows that permeability of a fracture depends on a large number of elements, all of which contribute to the ability of a fracture to provide a suitable flow path. The interaction of the proppant with the shale fracture downhole is an important factor for maintaining permeability and slowing crack closure.

This study provides empirical results consistent with published work on closure of a propped fracture in shale, and adds some mechanistic processes in support of the previous work. Observation of flow decrease with increasing time coupled with observations such as deformation of the host rock, deformation of the proppant, and fracture closure are effectively reducing the flow aperture; thereby decreasing the permeability of the fracture. The combination of mechanisms/processes results in an effective aperture decrease. This may be compared to a simple fracture closure model in future work.

In regards to the proppant itself there does not appear to be a reason why some proppant particles fractured while others did not in this testing other than their isolation from other particles. This means that an individual proppant particle could be carrying much more load; however, fractured particles were also observed in the middle of a proppant pillar, which is much harder to explain. It is likely due a combination of point loading conditions, grain to grain contacts (Hertzian), and the proppant not being distributed in a monolayer, but that has not been determined rigorously in this test.

In reference to the interaction of the proppant and the fracture wall, it appears that spalling of the walls of the fracture is a significant contributor to permeability loss. When these small pieces of shale combine with transport due to flow they cause significant flow restriction in regions where they tend to pack together (typically what appears to be a slight narrowing of the fracture aperture). This seems to be causing noteworthy reduction in the size of the flow paths as the test progresses.

Proppant embedment and clay swelling do not appear to be as significant of a problem with this particular combination of shale and quartz proppant, but it could be a much bigger problem in softer shale, or shale richer in swelling clays. Alternatively, it could also be that the embedment of the proppant in the shale required longer time scales than this test allowed.

These results qualitatively show that decreases in permeability due to fracture width decreases which are caused by imposed loads resulting in proppant failure, spalling of fracture surfaces, and proppant embedment. If these mechanisms are operative in the real world (and it would make sense that they are), then they are likely significant contributors to production declines in hydraulically fractured shale reservoirs. There are likely

more mechanisms that contribute to production decline, especially those which require more time to become apparent. However, the mechanisms shown herein likely have a significant contribution for long time scales considering their effect on short time scales.

6. ACKNOWLEDGEMENTS

Sandia National Laboratories is a multi-program laboratory managed and operated by Sandia Corporation, a wholly owned subsidiary of Lockheed Martin Corporation, for the U.S. Department of Energy's National Nuclear Security Administration under contract DE-AC04-94AL85000. SAND2015-XXXX

REFERENCES

1. Walsh, J.B. 1981. Effect of Pore Pressure and Confining Pressure on Fracture Permeability. *Int. J. Rock Mech. Min. Sci & Geomech. Abstr.*18: 429-435.
2. Gangi, A.F. 1978. Wariation of Whole and Fracture Porous Rock Permeability with Confining Pressure. *Int. J. Rock Mech. Min. Sci & Geomech. Abstr.*15:249-257.
3. Arthur, J.D., B. Bohm, M. Layne. 2008. Hydraulic Fracturing Considerations for Natural Gas Wells of the Marcellus Shale. Presented at: *The Ground Water Protection Council 2008 Annual Forum, Cincinnati, OH, USA, 21-24 June.*
4. Daneshy, A. 2005. Proppant Distribution and Flowback in Off-Balance Hydraulic Fractures. Presented at: *2004 SPE Annual Technical Conference and Exhibition. Houston, TX, USA, 26-29 September.*
5. Baihly, J., R Altman, R. Malpani, and F. Lao. 2010. Shale Gas Production Decline Trend Comparison Over Time and Basins. Presented at: *SPE Annual Technical Conference. Florence, Italy, 19-22 September.*
6. Samuelson, M.J., J. Stefanski, and R. Downie. 2012. Field Development Study: Channel Hydrauilc Fracturing Achieves Both Operational and Productivity Goals in the Barnett Shale. In *SPE Americas Unconventional Resources Conference, Pittsburgh, PA, USA, 5-7 June*.
7. Morris, J., and N. Chugunov. 2014. Comparison of Heterogeneously-Propped Hydraulic Fractures for Vertical and Lateral Wells. Presented at: *AGU Fall Meeting, 2014. San Francisco, CA, USA, 15-19 December.*
8. Wen, Q., S. Zhang, L. Wang, Y. Liu, X. Li. 2006. The effect of proppant embedment upon the long-term conductivity of fractures. *J. Pet. Sci. and Eng.* 55: 221-227.
9. Fredd, C.N., S.B. McConnell, C.L. Boney, K.W. England. 2000. Experimental Study of Hydraulic Fracture Conductivity Demonstrates the Benefits of Using Proppants. Presented at: *SPE Rocky Mountain Regional/Low Permeability Reservoirs Symposium, Denver, CO, USA, 12-15 March.*
10. Alramahi, B., M.I. Sundberg. 2012. Proppant Embedment and Conductivity of Hydraulic Fractures in Shales. Presented at: *46th US Rock Mechanics/Geomechanics Symposium, Chicago, IL, USA, 24-27 June.*